

An application of bio-degradable polymers for electrolyte inside Lithium ion batteries including (m, m) SWCNTs as anodic material

Marzieh Sadat Madani¹, Majid Monajjemi^{2,*}, Hossein Aghaei¹

¹Department of Chemistry, Science and Research Branch, Islamic Azad University, Tehran, Iran

²Department of Chemical engineering, Central Tehran Branch, Islamic Azad University, Tehran, Iran

*corresponding author e-mail address: m_monajjemi@srbiau.ac.ir

ABSTRACT

We report the stability and electronic structures of bio-degradable polymers as electrolyte inside Lithium ion batteries including various nanotubes carbon (SWCNTs) to interact with anodic materials. Lithium ion conducting polymer blend electrolyte films based on polyvinyl alcohol (PVA) and polyvinyl pyrrolidone (PVP) within SWCNT has produced a large potential as anodic-electrolyte material for lithium ion batteries due to their unique structural geometry, mechanical construction, and electrical properties. The measured reversible lithium ion of (m, m) SWCNTs// (Li⁺)_n/PVA and (m, m)SWCNTs// (Li⁺)_n/PVP are improved compared to the conventional graphite's-based/(Li⁺)_n/LiClO₄. In this work (5, 5), (7,7) and (10,10) SWCNTs as anode material to interact with bio-degradable polymers (PVA and PVP) have been investigated. Additionally, we have found the structure of (7, 7) SWCNTs can be to improve the capacity and electrical transport in anode-based LIBs with this kind of electrolytes.

Keywords: lithium ion battery; SWCNTs; PVA; PVP; bio-degradable polymers.

1. INTRODUCTION

LIBs generally consist of a (+) electrode, a (-) electrode and conducting electrolytes where store electrical energies in the two electrodes in the form of Li-intercalation compounds. Electrolytes, two electrodes, and separators are the main component of the lithium ion batteries where the two electrodes within interaction to electrolytes play an essential role in the efficiency of these kind batteries.

In the structure PVA and PVP electrolytes, the hydroxyl and carbonyl structures act as the pair electrons donor which enable complexation with lithium ion. Moreover, PVP and PVA both are important electrolytes because of film-forming properties, without toxic, cheap price, and other important items which are biodegradable. PVA is semi-crystalline macromolecules and its crystalline natures are reduced via an extra concentration from amorphous natures (PVP). Both of them are soluble in polar solvent such as DMSO with a high-degree complexation within the large variety of dopants.

During the discovery of reversible, Li-intercalation carbonaceous compounds and low-voltage battery, Sony's company discovered the commercialization of xC₆/Li_{1-x}CoO₂ cells in 1991 [1]. Lithium ion batteries (LIBs) are amazing energy storage devices for electrochemical energies, generally used in the small storage systems. The favorable electrochemical efficiency of LIBs regarding energies and power density, as well as in manufacturing of a cell designing, has made LIBs greatly successful for electronics instruments.

During LIBs charging, lithium ions released from the cathode through the electrolytes (PVP and PVA) which is a bio-degradable polymer and is important for interacting with the anodic (SWCNTs) compounds. Although those electrolytes establish a large ionic conductivity between SWCNTs electrodes,

the PVP and PVA are not related to the conduction of free electrons and so the electrons complete the half reactions via an extra moving in external wire. In discharging, the lithium ions are extracted from the SWCNTs and move back to the cathode.

SWCNTs presently are the most important molecules used for the anodic materials of batteries because of its capability for reversible lithium intercalation in the layered crystals [2].

There are no works for experimenting with the cylindrical nanotube to increase lithium storage capacity or improving recharging cyclic efficiency. There are many reviews on the anode carbon sheet [1-11] which most of them have focused on inorganic electrolyte compounds. By this work, a semi-empirical study and also first-principal investigation have been used for calculating the amount of lithium ion storages between SWCNTs and these kinds of electrolytes, as well as some heteroatom-substituted carbon materials [12-17].

Although a lot works have been made for finding the suitable replacement, currently only LiClO₄ and LiPF₆ are important and used for a commercial electrolyte which are much more dangerous for the environment and also are bio-degradable polymers in contrast of PVP and PVA. For those degradable polymers, there are no theoretical or experimental reports for these kind electrolytes in LIBs.

This work has investigated to find the suitable replacement for carbonaceous materials with interacting to PVP and PVA Fig.1. The efficiencies of LIB including cycle lives, power densities and energies densities are extremely influenced by electrolyte-anodic compounds. The items are including fast diffusivities of lithium ion into the PVP and PVA, critical changes in crystal structures of anodic material, required low potential of anode materials for supplying the high cell voltages with the

cathodes and capabilities of storing significant amounts of charges per unit mass.

Conduction in anode's material is complex due to continuous phase transformations and the formation of the PVP and PVA–electrolytes interphase (SEI) layer [18, 19]. In other words, conduction is strongly dependent upon the degree of bio-degradable polymers.

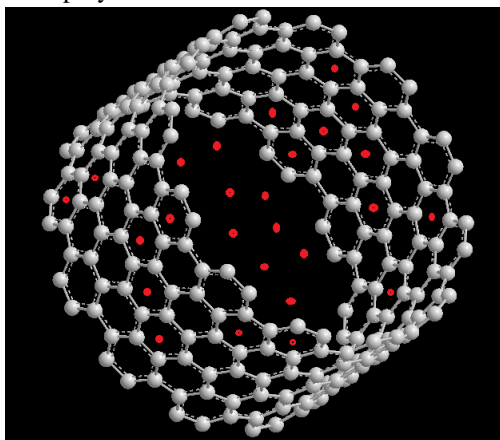


Fig. 1: Li⁺ intercalate with (7,7)SWCNTs.

The SWCNTs layer display much lower electronic and ionic conductivity compared to the bulk electrodes. The diffusion process can vary widely from grapheme sheet to SWCNTs materials [20-22]. SWCNTs have also been researched as an option to enhance electrochemical efficiency [21]. Although the nano-size diameter dimension and other superior material

2. EXPERIMENTAL SECTION

2.1. Li⁺ diffusivity in PVP and PVA electrolytes.

In contrast to graphite, CNTs are transparent and is an insulator. Electronic properties of CNTs and CNTs are radically different from each other and can be shown by theoretical calculations [28] for band structures of a single layer of CNT. For a single layer of graphite, a Graphene, two bands cross each other at fermi energy. In this study, charging and discharging of Li-ions has investigated in (m, m)SWCNTs with the positive electrode reaction as: $\text{LiCoO}_2 \rightleftharpoons \text{Li}_{1-x}\text{CoO}_2 + x \text{Li}^+ + x \bar{e}$ and the negative electrode reaction as: $x(7,7)\text{SWCNTs} + x \text{Li}^+ + x \bar{e} \rightleftharpoons x \text{Li}(7,7)\text{SWCNTs}$, while the whole reaction is: $\text{LiCoO}_2 + x(7,7)\text{SWCNTs} \rightleftharpoons \text{Li}_{1-x}\text{CoO}_2 + x \text{Li}(7,7)\text{SWCNTs}$. Recently many works have been investigated to describe the intercalation and diffusion of Li at different sites on CNTs and many studies have been performed in order to explain the mechanism by which lithium ions are stored in CNTs, including theoretical works (Fig.1). Yang *et al.* [24] imaged the surfaces mechanisms by which the naked surfaces of CNTs and are able for storing lithium species, via investigation of the electrochemical intercalation of lithium into PVA and PVP electrolytes. Both side (outside and inside) of the nanotubes are susceptible to lithium intercalations and achieved a high Li density.

2.1. Diffusion's mechanism in matrix.

Li⁺ diffusion determines some of the important keys performance metrics of Li-ion batteries cells (Fig.3), including the

properties of carbon nanotubes (CNTs) is suitable for anode materials, CNTs are not successful as anode materials [21, 22], due to the commercial electrolytes such as LiPF₆ (in contrast PVP or PVA). So, instead of grapheme the bio-degradable polymers as electrolyte inside Lithium ion batteries applied for electrolyte materials in LIBs.

Most, reports on Li-ion diffusivities adds improving measurement technique and not the diffusion mechanisms by themselves. This may derive from the various phase mixtures, the staging phenomenon of PVP and PVA, and the complexity caused by the solvents [20-23].

Using the cylindrical carbon materials as two electrodes including vacuum dielectric in anode and PVP electrolytes has been shown to increase cell performance by this work (Figs.2&3).

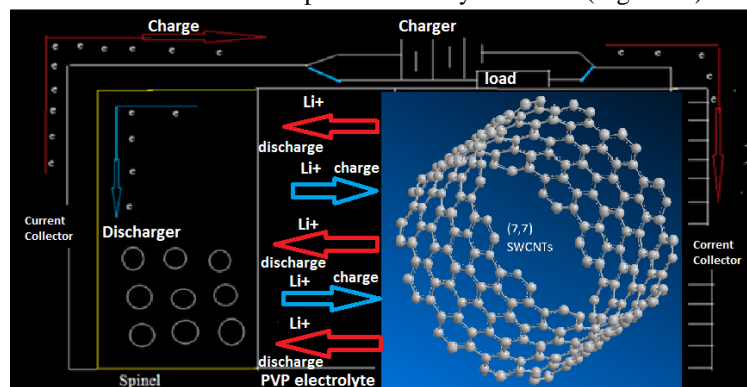


Fig. 2: Operating Li-ion battery including (7, 7) SWCNTs for diffusion Li⁺ into PVP electrolyte.

charge and discharge rates, practical capacities and cycling stabilities. The equations describing the diffusion process are known as Fick's law:

$$j_i = -D_i \nabla C_i \quad (1) \quad \text{And} \quad \frac{\sigma C_i}{\sigma t} = \nabla \cdot (D \nabla C_i) \quad (2)$$

which "j_i" is an ionic flux, molcm⁻² s⁻¹, D_i are diffusivities of solutes (PVP and PVA), cm² s⁻¹ [25]. Factors D are the diffusivities coefficient $D_i = \frac{k_B T}{6\pi\mu R_0}$ (3) [26, 27].

In PVP or PVA electrolytes, diffusions are governed through a random jump of Li+, leading to position exchange with their neighbors.

The kinetics of these mechanisms is temperature dependence $rate \approx \exp\left(-\frac{\Delta G}{k_B T}\right)$ (4) [25-27].

In PVP and PVA electrolytes, the temperature dependence of the diffusions is much less than in solids. (Eq. 2) [24-27].

Although the Li-ions are one of the smallest ions, they are still quite bigger when compared to an electron, the radius of a Li-ions are ten times larger than that of the electrons [25-27]. Also, the motion of a Li-ion is strongly barricaded via the potential created through the presence of adjacent ions. The van der Waals non-bonded forces, illustrated as the Lenard–Jones interaction, are strongly weak despite exhibiting a longer interaction range. In the case of the SWCNTs, the Li-ions can easily diffuse parallel rather than the graphite layer during intercalation. Thus in order to

understand the diffusion of the Li-ion, it is important to consider SWCNTs structures as well as the surrounding potentials.

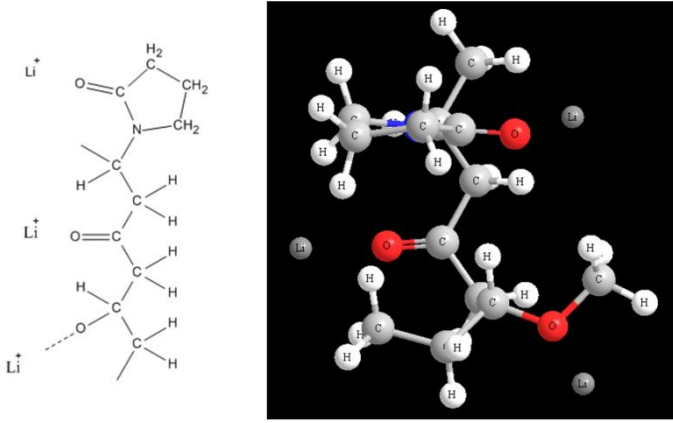


Fig. 3: Possible interaction between polymer PVP and Li⁺

2.2. Density energies of lithium in diffusion into PVP and PVA

(The electron densities have been defined as $\rho(r) = \sum_i \eta_i |\varphi_i(r)|^2 = \sum_i \eta_i \left| \sum_l C_{li} \chi_l(r) \right|^2$ (5). [28] Where η_i is orbital (i), φ are orbital wave functions, χ are basis functions. Atomic unit for electron density can be explicitly written as e/Bohr^3 . $\nabla\rho(r) = \left[\left(\frac{\partial\rho(r)}{\partial(x)} \right)^2 + \left(\frac{\partial\rho(r)}{\partial(y)} \right)^2 + \left(\frac{\partial\rho(r)}{\partial(z)} \right)^2 \right]^{\frac{1}{2}}$ (6) $\nabla^2\rho(r) = \frac{\partial^2\rho(r)}{\partial x^2} + \frac{\partial^2\rho(r)}{\partial y^2} + \frac{\partial^2\rho(r)}{\partial z^2}$ (7) [28].

The positive and negative values of these functions correspond to electron densities are locally depleted and locally concentrated respectively. The relationships between $\nabla^2\rho$ and valence shells electron pair repulsions, chemical bond type, electron localization and chemical reactivity have been exhibited by Bader [29].

The kinetic energy densities are uniquely defined as:

$$\langle \varphi | -\left(\frac{1}{2}\right) \nabla^2 | \varphi \rangle \quad (8). \text{ The general definitions are: } k(r) = -\frac{1}{2} \sum_i \eta_i \varphi_i^*(r) \nabla^2 \varphi_i(r) \quad (9) \text{ Relative to } K(r). \text{ The Lagrangian kinetic energy densities, "G(r)" is also known as: } G(r) = \frac{1}{2} \sum_i \eta_i |\nabla(\varphi_i)|^2 = \frac{1}{2} \sum_i \eta_i \left\{ \left(\frac{\partial\varphi_i(r)}{\partial(x)} \right)^2 + \left(\frac{\partial\varphi_i(r)}{\partial(y)} \right)^2 + \left(\frac{\partial\varphi_i(r)}{\partial(z)} \right)^2 \right\} \quad (10).$$

$K(r)$ and $G(r)$ are directly related by Laplacian of electron density $\frac{1}{4} \nabla^2 \rho(r) = G(r) - K(r)$ (11)

Becke [30] noted that spherically averaged conditional pair probabilities with the Fermi hole and then exhibited electron

localization function (ELF) [30]. $\text{ELF}(r) = \frac{1}{1 + [D(r)/D_0(r)]^2}$ (12)

where $D(r) = \frac{1}{2} \sum_i \eta_i |\nabla\varphi_i|^2 - \frac{1}{8} \left[\frac{|\nabla\rho_\alpha|^2}{\rho_\alpha(r)} + \frac{|\nabla\rho_\beta|^2}{\rho_\beta(r)} \right]$ (13) and

$D_0(r) = \frac{3}{10} (6\pi^2)^{\frac{2}{3}} [\rho_\alpha(r)^{\frac{5}{3}} + \rho_\beta(r)^{\frac{5}{3}}]$ (14) for close-shell system, since $\rho_\alpha(r) = \rho_\beta(r) = \frac{1}{2}\rho$, D and D_0 terms can be simplified as

$D(r) = \frac{1}{2} \sum_i \eta_i |\nabla\varphi_i|^2 - \frac{1}{8} \left[\frac{|\nabla\rho|^2}{\rho(r)} \right]$ (15), $D_0(r) = \frac{3}{10} (3\pi^2)^{\frac{2}{3}} \rho(r)^{\frac{5}{3}}$ (16).

Savin *has* reinterpreted the ELF [31], which makes a meaningful for Kohn-Sham DFT equations. They $D(r)$ reveals the excess kinetic energy densities caused by Pauli repulsions [32]. Localized orbital locators (LOL) are important function for locating high localization regions as the same ELF, defined by Schmider [33].

$$\text{LOL}(r) = \frac{\tau(r)}{1 + \tau(r)} \quad (17), \text{ where } \tau(r) = \frac{D_0(r)}{\frac{1}{2} \sum_i \eta_i |\nabla\varphi_i|^2} \quad (18).$$

2.3. Computational details

Based on some of our previous works our calculations have been done. [34-48].

In this work, we have mainly focused on getting the optimized results for each tube of SWCNTs from DFT methods including the m06 and m06-L. The m062x, m06-L, and m06-HF are strong Meta hybrid DFT functional in non-bonded calculations and are suitable for calculating the energies of the distance between tubes and electrolytes (PVA and PVP). Pm6, Extended-Huckel, and Pm3MM including pseudo=lan12z calculations using abinitio program have done for the non-bonded interaction between tubs and electrolytes.

M06 and m06-L (DFT) functionalism are based on an iterative solution of the Kohn-Sham equations [49] of those density functional theories in the plane-wave sets with the projector-augmented wave pseudo-potential. The Perdew-Burke-Ernzerhof (PBE) [50] exchange-correlation of the generalized gradient approximations (GGA) is adopted.

A fixed SWCNTs geometry with electrolytes of PVP and PVA and Li_x for various tubes is chosen with no further geometry optimization.

We further calculated the interaction energies between x lithium of the SWCNTs with electrolytes. The interaction energies were calculated via Mp6 methods in all items according to eq.19:

$$\Delta E_S (eV) = \{E_{total} - (E_{xLi} + E_{SWCNTs} + E_{PVP})\} + E_{BSSE} \quad (19)$$

Where the " ΔE_S " is the stability energy of system.

3. RESULT AND DISCUSSION

A listed data of density energies, electron localization functions (ELF), localized orbital locators (LOL) and local entropies including gap energies, charges from ESP, electrostatic potentials, ionization energies, the charges of (m, m)SWCNTs and the stability energies are shown in tables 1,2 and these data have been plotted in the figures (Figs.1-10). We have calculated the gradient norm and the Laplacian of electron densities via Eqs (5- 7) for the lithium diffused in the PVP and PVA electrolytes respectively.

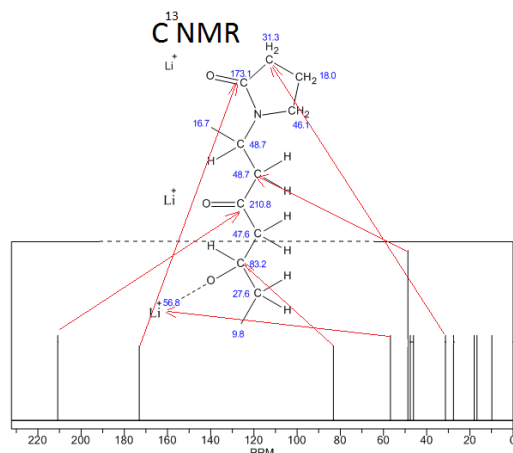
Table 1: Density, energy, Electron localization function (ELF), The localized orbital locator (LOL) and Local Entropy for each Li of 5 lithium Ion diffused on PVP & PVA.

Lithium No.	Density of all electron $\times 10^4$	Density of α electron $\times (10^4)$	Density of β electron $\times 10^4$	Potential energy density $\times 10^3 \text{ J}$	LOL $\times 10^3$	Local Entropy $\times 10^4$	Ellipticity	ELF $\times 10^7$	Ein index
PVP									
Li(1)	0.44	0.22	0.22	-0.18	0.19	0.37	-0.33	0.35	0.2
Li(2)	0.38	0.19	0.19	-0.23	0.18	0.55	-0.24	0.40	0.16
Li(3)	0.28	0.14	0.14	-0.29	0.22	0.52	-0.26	0.33	0.18
Li(4)	0.28	0.14	0.14	-0.21	0.24	0.56	-0.29	0.26	0.17
Li(5)	0.34	0.16	0.18	-0.32	0.21	0.44	-0.22	0.24	0.15
PVA									
Li(2)	0.38	0.19	0.19	-0.31	0.23	0.32	-0.28	0.32	0.16
Li(2)	0.22	0.11	0.11	-0.34	0.18	0.33	-0.31	0.33	0.19
Li(3)	0.35	0.17	0.18	-0.22	0.19	0.54	-0.23	0.40	0.16
Li(4)	0.34	0.17	0.17	-0.23	0.19	0.55	-0.23	0.39	0.16
Li(5)	0.38	0.19	0.19	-0.25	0.25	0.44	-0.24	0.38	0.14

Table 2: Gap energy, charge from ESP, electrostatic potential and Ionization energy for each Li of 5 lithium ion diffused on SWCNTs

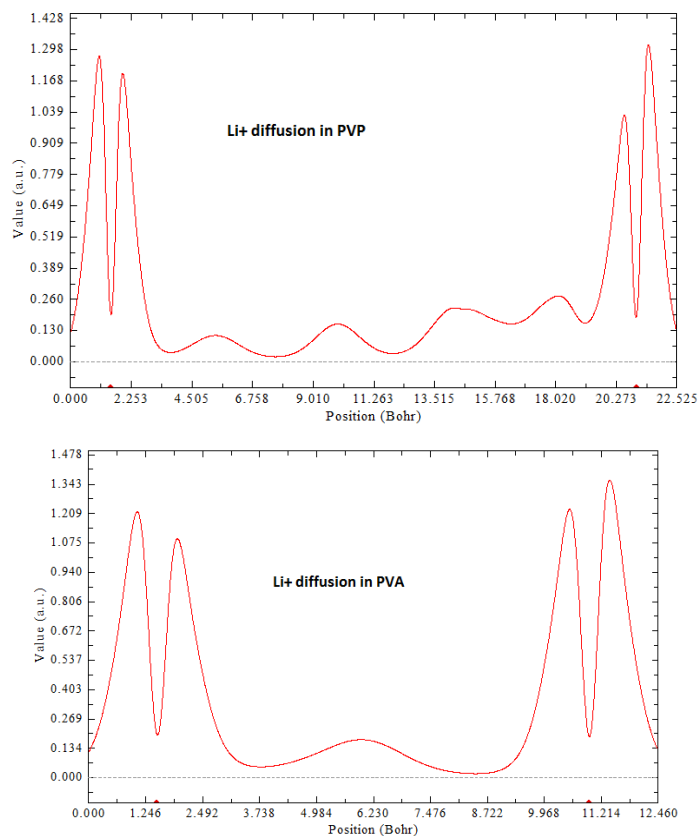
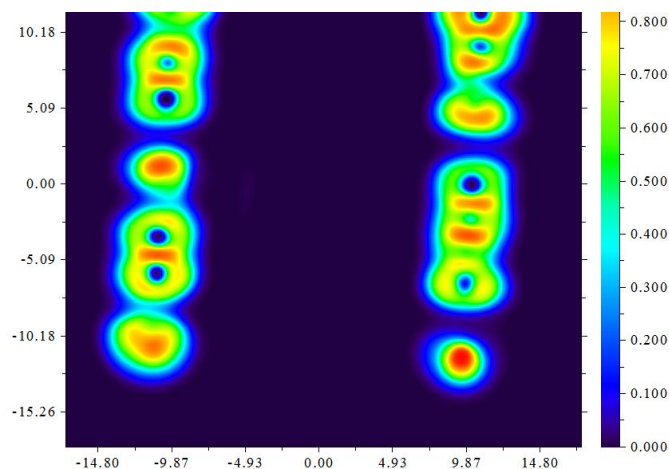
Lithium No.	Gap (Kj/mol)	Charge from ESP a.u.	Electrostatic Properties a.u.	Average Local Ionization Energy	Hole For $a \times 10^{-8}$
PVP					
Li(1)	0.037	0.90	-0.15	0.65	-0.12
Li(2)	0.035	0.99	-0.08	0.71	-0.32
Li(3)	0.033	0.98	-0.11	0.73	-0.40
Li(4)	0.042	0.96	-0.11	0.82	-0.18
Li(5)	0.043	0.99	-0.12	0.68	-0.45
PVA					
Li(1)	0.04	0.91	-0.13	0.66	-0.11
Li(2)	0.038	0.92	-0.12	0.64	-0.42
Li(3)	0.039	0.97	-0.09	0.63	-0.24
Li(4)	0.033	0.96	-0.09	0.62	-0.22
Li(5)	0.039	0.99	-0.13	0.61	-0.25

For calculation the electron spin densities from the difference between alpha and beta densities, we have Used $\rho^s(r) = \rho^\alpha(r) - \rho^\beta(r)$ then the spin polarization parameter functions will be returned instead of spin densities $\xi(r) = \frac{\rho^\alpha(r) - \rho^\beta(r)}{\rho^\alpha(r) + \rho^\beta(r)}$. The kinetic energy densities, Lagrangian kinetic energy densities, and the electrostatic potential from nuclear / atomic charges can be calculated as eqs. (9), (10) and: $V_{nuc}(r) = \sum_A \frac{Z_A}{|r - R_A|}$ where RA and ZA denote position vector and nuclear charge of atom A, respectively and are listed in tables 1, 2.


Fig. 4. C13NMR of PVP.

Bader found that the regions which have large electron localization must have large magnitudes of Fermi hole integrations. However, the Fermi holes are a six-dimension function and thus difficult to be studied visually.

Since $D_0(\mathbf{r})$ from eqs 11-16 is introduced into ELF as references, what the ELF reveals is exactly a relative localization {ELF is within the range of [0, 1]}. A large ELF value indicates that electrons are greatly localized, indicating that the PVP and PVA are suitable interface electrolyte for Li+ diffusion. ELF's have been widely used for the wide varieties of systems, such as organic and inorganic small molecules, atomic crystals, coordination compounds, clusters, and for different problems, such as the revealing atomic shell structure, classification of chemical bonding, verification of charge-shift bond, studying aromaticities.


Fig. 5: The Ddensity of electron changes for Li+ diffusion on PVP and PVA versus distance.

Fig. 6: ELF anode and cathode situation with PVP electrolyte.

In which the actual kinetic energies term in $D(\mathbf{r})$ from eqs. 15-16 is replaced by Kirzhnits type second-order gradient that is $\frac{1}{2} \sum_i \eta_i |\nabla \phi_i|^2 \approx D_0(r) + \frac{1}{72} \frac{|\nabla \rho|^2}{\rho(r) + \frac{1}{6} \nabla^2 \rho(r)}$ (20) so that ELF's are totally independent from wave-function, and then can be used to analyze electron densities from X-ray diffraction data. Of course Tsirelson ELF can also be used to analyze electron densities from quantum chemistry calculations, but is not as good as the ELF defined by Becke owing to the approximation introduced in kinetic energies term.

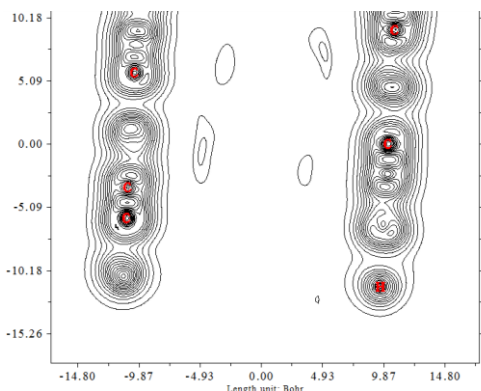


Fig. 7: LOL Contour line map of two electrodes with PVA electrolyte.

LOLs have similar definition compared to ELF. Actually, the chemical regions that highlighted by the LOLs and ELFs are basically qualitative comparable, while Jacobsen pointed out which LOLs conveys more deceives and clearer the pictures than ELFs, Obviously LOLs can be interpreted in kinetic energies way as for ELFs; however LOLs can also be interpreted in view of localized orbitals.

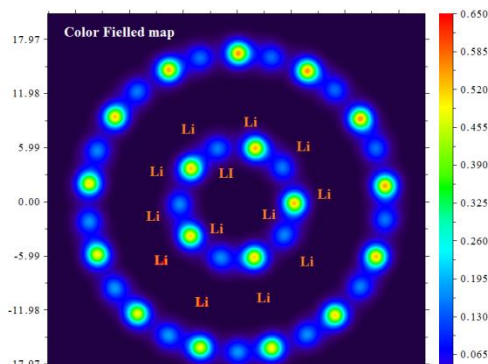


Fig. 8: Color Filled map of (5,5)@(7,7)SWCNTs including Li atoms.

In this work, we have calculated the interaction energies between SWCNTs and those electrolytes (PVP and PVA) for each lithium ions via eqs. 19.

As lithium has a single electron in the last orbital, leading to a difference in spin-up and spin-down, when two lithium atoms are adsorbed simultaneously electrons get paired and magnet

4. CONCLUSION

Increasing oil difficulties estimates that by 2020, hybrid vehicles are to account for more than 10% of the global transportation markets. Growing of hybrid vehicles is driving the global demand for lithium ion batteries but what about when those vehicles reach the end of usage? Is it possible for Li-ion easily recycling of this instrument? The rechargeable batteries recycling

5. REFERENCES

[1] Yang Z.-G., Zhang J.-L., Kintner-Meyer M.C.W., Lu X.-C., Choi D.-W., Lemmon J.P., Liu J., Electrochemical energy storage for green grid, *Chem. Rev.*, 111, 3577–3613, **2011**.
 [2] Guerard D, Herold A, Intercalation of lithium on to Graphene and other carbons, *1975*, 13, 337-345, **1975**.
 [3] Yoo E.J, Kim J., Hosono E., Zhou H.S., Kudo T., Large reversible Li storage of graphene nanosheet families for use in rechargeable lithium ion batteries, *Nano. Lett.*, 8, 2277-2282, **2008**.
 [4] Wang G., Shen X.P., Yao J., Park J., Graphene nanosheets for enhanced lithium storage in lithium ion batteries. *Carbon*, 47, 2049-2053, **2009**.

moment disappears. So, spin polarized clusters have some gaps which size depends on adsorbed electron spin polarization.

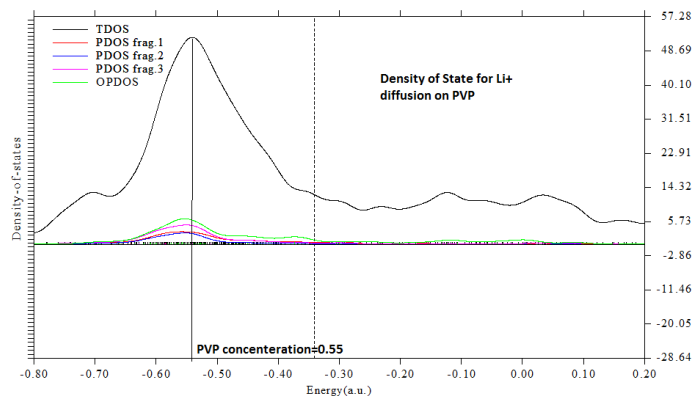


Fig. 9: TDOS, PDOS and OPDOS of (7, 7) SWCNTs for Li⁺ diffusion on PVP.

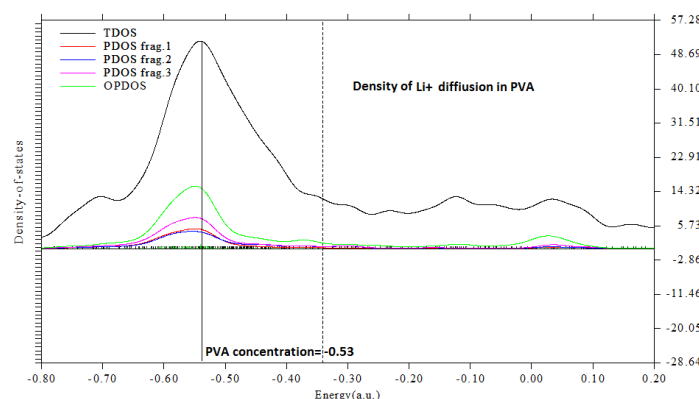


Fig. 10: TDOS, PDOS and OPDOS of (7, 7) SWCNTs for Li⁺ diffusion on PVA.

In this work, we have shown SWCNTs does demonstrate high performance with PVP and PVA electrolytes, good mechanical strengths, excellent flexibilities, great chemical stabilities and high surfaces. This is especially noticeable when SWCNTs are converted with PVP and PVA electrolytes, proving that it is suited for use as a base composite electrode material.

is the most challenges for new worlds especially the electrolyte of these batteries are dangerous for environments. Via this work, it has been exhibited that the PVA and PVF are suitable electrolytes for lithium ion batteries in view oint of 1-increasing the efficiency of the voltage and amperage and 2-They are bio-degradable polymers electrolyte which are suitable for ecology.

[5] Bhardwaj T., Antic A., Pavan B., Barone V., Fahiman B.D., Enhanced electrochemical lithium storage by graphene nano-ribbons, *JACS*, 132, 12556-12558, **2010**.
 [6] Suzuki T., Hasegawa T., Mukai S.R., Tamon H., A theoretical study on storage states of Li ions in carbon anodes of Li ion batteries using molecular orbital calculations, *Carbon*, 41, 1933-1939, **2003**.
 [7] Monajjemi M., Non-covalent attraction of B2N (-,0) and repulsion of B2N(+) in the BnNn ring: a quantum rotatory due to an external field *Theoretical chemistry accounts*, 134, 6, 1-22, **2015**
 [8] Noel M., Suryanarayanan V., Role of carbon host lattices in Li-ion intercalation/de-intercalation processes, *Journal of Power Sources*, 111, 193–209, **2002**.

- [9] Tirado J.L., Inorganic materials for the negative electrode of lithium-ion batteries: state-of-the-art and future prospects, *Materials Science and Engineering R 40*, 103–136, **2003**.
- [10] Fu L.J., Liu H., Li C., Wu Y.P., Rahm E., Holze R., Wu H.Q., Surface modifications of electrode materials for lithium ion batteries *Solid State Sciences*, 8, 113–128, **2006**.
- [11] Frackowiak E., Béguin F., Electrochemical storage of energy of energy in carbon nanotubes and nano structured carbons, *Carbon*, 40, 1775–1787, **2002**.
- [12] Monajjemi M., Non bonded interaction between BnNn (stator) and BN(-,0,+)B (rotor) systems: A quantum rotation in IR region, *Chemical Physics*, 425, 29–45, **2013**
- [13] Safran S.A., Hamann D.R., Long-Range Elastic Interactions and Staging in Graphite Intercalation Compounds, *Physical Review Letters*, 42, 21, 1410–1413, **1979**.
- [14] Monajjemi M., Chegini H., Mollaamin F., et al. Theoretical Studies of Solvent Effect on Normal Mode Analysis and Thermodynamic Properties of Zigzag (5,0) Carbon Nanotube, *Fullerens Nanotubes carbon and nanostructures*, 19, 5, 469–482, **2011**.
- [15] Peter M. Levy., Morin P., Schmitt D., Large Quadrupolar Interactions in Rare-Earth Compounds *Phys. Rev. Lett.* 42, 1417, **1979**
- [16] Monajjemi M., Baei M. T., Mollaamin F. Quantum mechanics study of hydrogen chemisorptions on nanocluster vanadium surface, 53, 9 1430–1437, *RUSSIAN JOURNAL OF INORGANIC CHEMISTRY* **2008**.
- [17] Lee J.K., An K.W., Ju J.B., Cho B.W., Cho W.I., Park D., Yun K.S., Electrochemical Properties of Pan-Based Carbon Fibers as Anodes for Rechargeable Lithium Ion Batteries, *Carbon*, 39, 1299–1305, **2001**.
- [18] Ehrlich G.M., in: David Linden, (Ed.), *Handbook of Batteries*, 3rd ed., McGrawHill, 35.16–35.21, **2002**.
- [19] Churikov A.V., Gridina N.A., Churikova N.V., *New Carbon Based Materials for Electrochemical Energy Storage Systems*, Springer, 269–276, **2006**.
- [20] Naoi K., Ogihara N., Igarashi Y., Kamakura A., Kusachi Y., Utsugi K., New Materials and New Configurations for Advanced Electrochemical Capacitors, *Journal of the Electrochemical Society*, 152, 6, A1047–A1053, **2005**.
- [21] Monajjemi M., Faham R., Mollaamin F., Ab initio Study of Direct Diffusion Pathway for H⁺, Li⁺, Na⁺, K⁺ Cations into the (3,3), (4,4), and (5,5) Open-Ended Single-Walled Carbon Nanotubes *Fullerens Nanotubes carbon and carbon nanostructures* 20, 2, 163–169, **2012**
- [22] Endo M., Nishimura Y., Takahashi T., Takeuchi K., Dresselhaus M.S., Lithium storage behavior for various kinds of carbon anodes in Li ion secondary battery, *Journal of Physics and Chemistry of Solids*, 57, 6–8, 725–728, **1996**.
- [23] S. Chandrashekar, S., Nicole M., et al. Li MRI of Li batteries reveals location of microstructural lithium. *Nature Materials*, 11(7):311–315, **2012**.
- [24] Yang Z.-H.; Wu H.-Q., electrochemical interaction of lithium into raw carbon nanotubes, *Mater. Chem. Phys.*, 71, 7–11, **2001**.
- [25] Wilkinson D.S., Mass Transport in Solid and Fluids, *Cambridge University Press*, **2000**.
- [26] Mehrer H., Diffusion in Solids, *Springer*, 27–36, **2007**.
- [27] Porter D.A., Easterling K.E., *Phase Transformations in Metals and Alloys*, 2nd edition, Chapman & Hall, 1–109, **1992**.
- [28] Lu T., Chen F., Multiwfn: A Multifunctional Wavefunction Analyzer, *J. Comp. Chem.*, 33, 580–592, **2012**.
- [29] Bader R.F.W, *atoms in Molecule: A quantum Theory* (Oxford Univ. press, Oxford, **1990**.
- [30] Becke, Edgecombe, A simple measure of electron localization in atomic and molecular systems, *J. Chem. Phys.*, 92, 5397, **1990**.
- [31] Savin et al *Angew.*, *Chem. Int. Ed. Engl.*, 31, 187.
- [32] Tsirelson, Stash, *Chem. Phys. Lett.*, 351, 142.
- [33] Schmider, Becke, *J. Mol. Struct.*, (THEOCHEM), 527, 51.
- [34] Monajjemi M., Lee V.S., Khaleghian M., Honarparvar, B., Mollaamin F., Theoretical Description of Electromagnetic Nonbonded Interactions of Radical, Cationic, and Anionic NH₂BHNBNH₂ Inside of the B18N18 Nanoring, *J. Phys. Chem C*, 114, 15315, **2010**.
- [35] Monajjemi M., Quantum investigation of non-bonded interaction between the B15N15 ring and BH₂NBH₂ (radical, cation, and anion) systems: a nano molecular motor, *Struct Chem.*, 23, 551–580, **2012**.
- [36] Monajjemi M., Boggs J.E., A New Generation of BnNn Rings as a Supplement to Boron Nitride Tubes and Cages, *J. Phys. Chem. A*, 117, 1670–1684, **2013**.
- [37] Monajjemi M., Khaleghian M., EPR Study of Electronic Structure of [CoF₆](3-) and B18N18 Nano Ring Field Effects on Octahedral Complex, *Journal of Cluster Science*, 22, 4, 673–692, **2011**.
- [38] Monajjemi M.; Wayne Jr., Robert. Boggs J.E., NMR contour maps as a new parameter of carboxyl's OH groups in amino acids recognition: A reason of tRNA-amino acid conjugation, *Chemical Physics*, 433, 1–11, **2014**.
- [39] Monajjemi M., Falahati M., Mollaamin F., Computational investigation on alcohol nanosensors in combination with carbon nanotube: a Monte Carlo and ab initio simulation, *Ionics*, 19, 155–164, **2013**.
- [40] Mollaamin F.; Monajjemi M., DFT outlook of solvent effect on function of nano bioorganic drugs, *Physics and Chemistry of Liquids*, 50, 5, 596–604, **2012**.
- [41] Monajjemi M., Khosravi M., Honarparvar B., Mollaamin F., Substituent and Solvent Effects on the Structural Bioactivity and Anticancer Characteristic of Catechin as a Bioactive Constituent of Green Tea, *International Journal of Quantum Chemistry*, 111, 2771–2777, **2011**.
- [42] Monajjemi M., *Journal of Molecular Modeling*, 20, 2507, **2014**.
- [43] Monajjemi M., Khaleghian M., Mollaamin F., Theoretical study of the intermolecular potential energy and second virial coefficient in the mixtures of CH₄ and Kr gases: a comparison with experimental data, *Molecular Simulation*, 36, 11, 865–, **2010**.
- [44] Ilkhani Ali R., Monajjemi M., The pseudo Jahn-Teller effect of puckering in pentatomic unsaturated rings C(4)AE(5), A = N, P, As, E = H, F, Cl, *Computational and Theoretical Chemistry*, 1074, 19–25, **2015**.
- [45] Monajjemi M., Cell membrane causes the lipid bilayers to behave as variable capacitors: A resonance with self-induction of helical proteins, *Biophysical Chemistry*, **2015** 207, 114–127
- [46] Jalilian H., Monajjemi M., Capacitor simulation including of X-doped graphene (X = Li, Be, B) as two electrodes and (h-BN)(m) (m=1–4) as the insulator, *Japanese Journal of Applied Physics*, 54, 8, 08510, **2015**.
- [47] Mahdavian L., Monajjemi M., Alcohol sensors based on SWNT as chemical sensors: Monte Carlo and Langevin dynamics simulation, *Microelectronics Journal*, 41, 2–3, 142–149, **2010**.
- [48] Monajjemi M*, Bagheri S., Matin S. Moosavi, et al. Symmetry Breaking of B₂N(-,0,+): An Aspect of the Electric Potential and Atomic Charges, *Molecules*, 20, 21636–21657, **2015**.
- [49] Kohn W., Sham L.J., Self-Consistent Equations Including Exchange and Correlation Effects, *Phys. Rev.*, 140 A, 1133–1138, **1965**.
- [50] Perdew J.P., Burke K., Ernzerhof, Generalized Gradient Approximation Made Simple, *Phys. Rev. Lett.*, 77, 3865–3868, **1996**.

6. ACKNOWLEDGEMENTS

We are thanks the science and research branch of Azad University for helping us in bioinformatics center.

© 2018 by the authors. This article is an open access article distributed under the terms and conditions of the Creative Commons Attribution license (<http://creativecommons.org/licenses/by/4.0/>).